

## Research Paper

# ATP-activated decrosslinking and charge-reversal vectors for siRNA delivery and cancer therapy

Zhanwei Zhou<sup>1</sup>, Qingyan Zhang<sup>1</sup>, Minghua Zhang<sup>1</sup>, Huipeng Li<sup>1</sup>, Gang Chen<sup>1</sup>, Chenggen Qian<sup>1</sup>, David Oupicky<sup>1,2</sup>✉, Minjie Sun<sup>1</sup>✉

1. State Key Laboratory of Natural Medicines, Department of Pharmaceutics, China Pharmaceutical University, 24 Tong Jia Xiang, Nanjing 210009, P. R. China  
2. Center for Drug Delivery and Nanomedicine Department of Pharmaceutical Sciences University of Nebraska Medical Center Omaha, NE 68198, USA

✉ Corresponding authors: Prof. Minjie Sun, Phone /Fax: +86 25 83271098, Email: msun@cpu.edu.cn and Prof. David Oupicky, E-mail: david.oupicky@unmc.edu

© Ivyspring International Publisher. This is an open access article distributed under the terms of the Creative Commons Attribution (CC BY-NC) license (<https://creativecommons.org/licenses/by-nc/4.0/>). See <http://ivyspring.com/terms> for full terms and conditions.

Received: 2018.04.25; Accepted: 2018.07.17; Published: 2018.09.09

## Abstract

Stimuli-responsive polycations have been developed for improved nucleic acid transfection and enhanced therapeutic efficacy. The most reported mechanisms for controlled release of siRNA are based on polyelectrolyte exchange reactions in the cytoplasm and the degradation of polycations initiated by specific triggers. However, the degradation strategy has not always been sufficient due to unsatisfactory kinetics and binding of cationic fragments to siRNA, which limits the gene silencing effect. In this study, a new strategy that combines degradation and charge reversal is proposed.

**Methods:** We prepared a polycation (CrossPPA) by crosslinking of phenylboronic acid (PBA)-grafted 1.8k PEI with alginate. It was compared with 25k PEI, 1.8k PEI and 1.8k PEI-PBA on siRNA encapsulation, ATP-responsive behavior and mechanism, cytotoxicity, cell uptake, siRNA transfection, *in vivo* biodistribution and *in vivo* anti-tumor efficacy. The *in vitro* and *in vivo* experiments were performed on 4T1 murine breast cancer cells and 4T1 tumor model separately.

**Results:** The crosslinking strategy obviously improve the siRNA loading ability of 1.8k PEI. We validated that intracellular levels of ATP could trigger CrossPPA disassembly and charge reversal, which resulted in efficient and rapid siRNA release due to electrostatic repulsion. Besides, CrossPPA/siRNA showed strong cell uptake in 4T1 cells compared with 1.8k PEI/siRNA. Notably, the cytotoxicity of CrossPPA was pretty low, which was owing to its biodegradability. Furthermore, the crosslinked polyplexes significantly enhanced siRNA transfection and improved tumor accumulation. The high gene silencing ability of CrossPPA polyplex led to strong anti-tumor efficacy when using Bcl2-targeted siRNA.

**Conclusion:** These results indicated that the ATP-triggered disassembly and charge reversal strategy provided a new way for developing stimuli-responsive siRNA carriers and showed potential for nucleic acid delivery in the treatment of cancer.

Key words: ATP-responsive, charge reversal, phenylboronic acid, siRNA delivery, cancer therapy

## Introduction

RNAi technology has attracted tremendous interest among academic and industry investigators for its potential to treat many serious diseases [1]. Successful delivery vectors must be able to transport siRNA to the target site effectively and unload the cargo timely [2].

In non-viral gene delivery, cationic polymers are generally used to form polyplexes with negatively charged siRNA by electrostatic interactions [3]. However, polymer/siRNA polyplexes are thermody-

namically stable, which greatly weaken the gene silencing efficiency because only the released siRNA could silence the target protein [4, 5]. Hence, maintaining the balance between effective siRNA loading and controlled release plays a critical role in developing a siRNA delivery system. Many strategies have been utilized to facilitate controlled intracellular release of siRNA, including preparing stimulus-responsive polymers that degrade into fragments and therefore lower the charge density [6, 7, 8]. Although

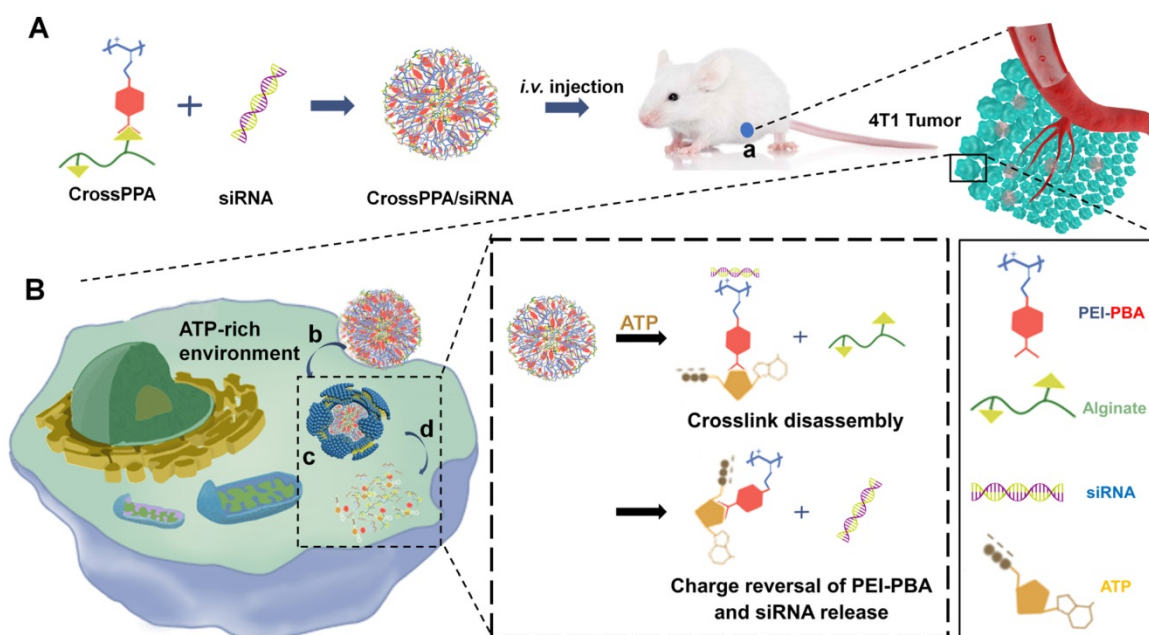
this strategy could accelerate the release of siRNA, positive groups remaining in the short chains still interact with siRNA and affect gene silencing. In this study, a crosslinked cationic polymer was developed that could degrade into short fragments and achieve fast charge reversal from positive to negative with the stimulus of ATP (adenosine triphosphate) in the cytosol.

ATP, the most abundant ribonucleotide in cells, provides energy for cellular proliferation and metabolism [9]. ATP is present in low concentrations (<0.4 mM) in the extracellular environment, but it is relatively concentrated within the cytosol (1–10 mM) [10–13]. Therefore, the intra/extracellular gradient of ATP inspired researchers to use it as a trigger for ATP-responsive nanocarriers [14, 15]. Prof. Kataoka's group reported PBA-functionalized polyion complex (PIC) micelles for ATP-triggered release of siRNA. In that study, ATP was used as a trigger for breaking up the borate ester bond between PBA and siRNA and therefore promoting siRNA release [14]. As we know, the negatively charged phosphate group in ATP also shows potential for drug delivery system design in tumor therapy. In this work, we desired to study the role of ATP's negative charge on triggering siRNA release. The pKa of ATP's primary and secondary phosphate groups are 1–2 and 6.5, respectively [16, 17] and the cytosol pH in tumor cells is around 6.8–7.2 [18, 19]. Hence, the ATP is negatively charged in the biological environment (both intracellular and intracellular space).

ATP maintains negative charge in the cytosol, which further gave us the evidence that ATP binding

in cytosol could reverse the carrier's zeta potential from positive to negative and should bring about the disassembly of polyplexes. The charge repulsion could trigger release of negatively charged therapeutic agent (such as siRNA, DNA or protein) from a cationic carrier. ATP, glucose and fructose were reported to have a unique ability to quickly form a boronic ester bond by dynamic chemical reaction with phenylboronic acid (PBA) due to their cis-1,2- or -1,3-diols [20, 21]. The binding between saccharides and PBA is highly sensitive to pH [22], other sugars [23], and H<sub>2</sub>O<sub>2</sub> [24, 25], making PBA moieties a suitable choice in stimuli-responsive drug delivery systems.

Taking these properties into consideration, we explored a crosslinked polymer based on PBA and saccharides, which was designed to remain stable in the blood circulation and disassemble in the cytosol by high intracellular concentration of ATP. The rapid rate of the reaction between PBA and ATP could accelerate the ATP binding progress and assist the disassembly of the polyplexes. The condensed negatively charged ATP around the polycations would reverse the charge from positive to negative, finally resulting in fast release of siRNA from carriers in the cytosol (**Scheme 1**). In addition, it has been reported that phenylboronic acid-modified nanoparticles can significantly enhance the tumor targeting delivery of anti-cancer drugs/gene, due to reaction of PBA with sialic acid (SA) over-expressed on the tumor cells [26, 27]. Therefore, PBA shows potential to be used as a ligand for tumor targeting in this study.



**Scheme 1.** (A) Schematic illustration of the formation of ATP-responsive charge reversal crosslinked polyplex. (B) Schematic illustration of tumor-targeted siRNA delivery by CrossPPA/siRNA polyplex: (a) tumor accumulation of CrossPPA/siRNA through passive and active targeting; (b) cell uptake of polyplex mediated by sialic acid; (c) endosomal escape of polyplex; (d) ATP-activated decrosslinking and charge reversal of CrossPPA, leading to siRNA release in the cytosol.

Herein, alginate was used as the diol linker to prepare crosslinked cationic polymers (CrossPPA) by forming borate esters between PBA and alginate. Low molecular weight polyethyleneimine (PEI 1.8k) was chosen as the cationic component for its low cytotoxicity. The crosslinking strategy condensed the charge of PEI 1.8k, improving its siRNA loading ability. PBA modification promoted cellular uptake and tumor targeting of the polyplex. Furthermore, intracellular ATP selectively triggered the release of siRNA. We also demonstrated a new mechanism of siRNA release from PBA-diol crosslinked polycations undergoing disassembly and charge reversal. The role of ATP's diols and phosphate group in accelerated siRNA release was clarified in this study. The crosslinked polyplexes effectively protected the siRNA from degradation in the serum, targeted the tumor, and released the cargo selectively in the cytosol. Our work demonstrated stimulus-responsive gene release by the combination of degradation and charge reversal, which shows strong potential for *in vivo* siRNA delivery and tumor therapy.

## Methods

### Materials, cell culture and animals

Branched polyethyleneimine (1.8k PEI and 25k PEI), alginate (270 kDa), 4-carboxyphenylboronic acid (PBA) and EDC.HCl (1-ethyl-3-(3-dimethylamino-propyl) carbodiimide hydrochloride) were purchased from Aladdin chemical reagent company (Shanghai, China). Trypsin EDTA solution, penicillin streptomycin solution, RPMI-1640 medium and MTT were purchased from KeyGen biotech (Nanjing, China). The Annexin V-FITC/PI Apoptosis Detection Kit (Cat No.40302) and Super ECL Detection Reagent (Cat No.36208) were bought from Yeasen company (Shanghai, China). Fetal bovine serum (FBS) was purchased from Gibco (Thermo Fisher Scientific, USA).

siNC (negative control), FAM-siNC, cy3-siNC, siLuc (targeting luciferase) and siBcl2 (targeting Bcl2) were synthesized by GenePharma (Shanghai, China). Cy5-siNC was synthesized by RiboBio (Guangzhou, China). Bcl2-specific antibody (50E3) rabbit mAb,  $\beta$ -tubulin (9F3) rabbit mAb and HRP-linked anti-rabbit IgG were purchased from Cell Signaling Technology. The siRNA sequences are below:

siNC, sense strand, 5'-UUC UCC GAA CGU GUC ACG UTT-3'

siLuc, sense strand, 5'-GGA CGA GGA CGA GCA CUU CUU-3'

siBcl2, sense strand, 5'-GCA UGC GAC CUC UGU UUG AdTdT-3'

4T1 mouse breast cancer cells were obtained

from ATCC (American Type Culture Collection). Female BABL/c mice (18-22 g) were bought from Yangzhou University. All the animal experiments were performed in compliance with the Guide for Care and Use of Laboratory Animals and were approved by China Pharmaceutical University.

### Synthesis and characterization of PEI-PBA

4-Carboxyphenylboronic acid was conjugated to branched PEI 1.8k via amide bonds using carbodiimide chemistry. Briefly, 50 mg of 4-carboxyphenylboronic acid was dissolved in 10 mL mixture solvent ( $\text{CH}_3\text{CH}_2\text{OH}:\text{H}_2\text{O} = 1:1$  v:v). Then, 200 mg of EDC.HCl was added into the mixture and reacted at room temperature for 1 h. The resultant solution was dropped into 100 mg of PEI 1.8k solution and kept stirring at room temperature for 24 h, followed by dialysis (MWCO = 1000 Da) against distilled water to obtain purified PEI-PBA. The chemical structure of PEI-PBA was characterized by  $^1\text{H-NMR}$ ,  $^{13}\text{C-NMR}$  spectra and FTIR. The PBA substitution degree was calculated based on the ratio of phenyl on PBA to the primary amine on PEI by the  $^1\text{H-NMR}$  result.

### Preparation of cross-linked polycations

CrossPPA (PEI-PBA-Alginate) was prepared based on borate ester formation between the PBA group on PEI-PBA and the diol group on alginate. The conjugation between PBA and diol was performed in neutral aqueous medium without any catalyst. A typical procedure is described as follows: PEI-PBA and alginate (PEI-PBA/alginate w/w ratios of 40:1, 20:1, 10:1, 5:1, 2.5:1 were optimized by luciferase silencing on 4T1 cells) were dissolved in HEPES buffer (pH 7.4) and stirred overnight at room temperature. The product was dialyzed (MWCO 1,000 Da) against distilled water for 48 h. Then, the CrossPPA polymer was lyophilized and stored at  $-20^\circ\text{C}$  for further preparation.

### Formulation of siRNA polyplexes

siRNA solution (40  $\mu\text{g}/\text{mL}$  in 10 mM HEPES, pH 7.4) was mixed with different concentration of polycations (25k PEI, 1.8k PEI, PEI-PBA and CrossPPA) to optimize the desired PEI/siRNA (w/w) ratios (w/w ratio means weight of PEI / weight of siRNA in the polyplex), where 1, 2, and 4 ratios were chosen for research. The w/w ratios of 1, 2, and 4 were equal to N/P of 7.4, 14.8, and 22.2. The mixture was vigorously vortexed for 30 s and incubated at room temperature for 30 min prior to use.

To evaluate polyplex formation, the polyplexes at w/w ratios of 0, 0.2, 0.5, 1, 2, and 5 were run on a 1% (w/v) agarose gel containing GelRed at 100 V for 15 min and siRNA was visualized by UV illumination.

The w/w ratios of 0, 0.2, 0.5, 1, 2, and 5 were equal to N/P of 0, 1.48, 3.7, 7.4, 14.8, and 22.2.

Particle size and zeta potential of the siRNA polyplexes were determined by a dynamic light scattering (DLS) analyzer (Brookhaven) and a ZetaPlus zeta potential analyzer (Brookhaven). The polyplexes were prepared at different w/w ratios (1, 2, 4) and diluted with 10 mM HEPES; the siRNA concentration was 5 µg/mL.

### ATP-responsiveness of PEI-PBA and CrossPPA polyplex

ATP-triggered release of siRNA from the polyplex was evaluated by agarose gel electrophoresis. siRNA-loaded polyplexes of 25k PEI, 1.8k PEI, PEI-PBA and CrossPPA were prepared at a w/w ratio of 4:1. After 30 min, each polyplex solution was divided into 2 parts, which were treated with 5 mM ATP or without ATP treatment, followed by agarose gel electrophoresis analysis immediately. To evaluate whether the siRNA release was time and ATP concentration dependent, each polyplex solution was treated with various concentrations of ATP (0 mM, 0.4 mM, 1 mM, 5 mM) and monitored at time intervals (0, 5, 10, 20, 40, 60, 90, 120 min) by Ribogreen assay [28]. For the release mechanism study, 5 mM dATP or adenosine were also incubated with PEI-PBA and CrossPPA polyplexes, followed by agarose gel electrophoresis analysis. The selectivity of PEI-PBA and CrossPPA polyplexes response to ATP in the cell, rather than phosphate and glucose in the blood, was also validated by incubation with 10 mM PBS (pH 7.4) containing 5 mM glucose for different times and was detected by agarose gel electrophoresis.

The morphological observations of CrossPPA/siRNA before and after 5 mM ATP treatment were obtained by H-600 transmission electron microscope (TEM) (Hitachi, Japan) after negative staining with 0.1 wt% sodium phosphotungstate solution.

The charge reversal of polycations and polyplexes after ATP incubation was measured using Zeta Plus. Different polycations of 25k PEI, 1.8k PEI, PEI-PBA and CrossPPA, polyplexes (w/w 4:1) of 25k PEI/siRNA, 1.8k PEI/siRNA, PEI-PBA/siRNA and CrossPPA/siRNA were respectively prepared in 10 mM HEPES solution with a PEI concentration of 200 µg/mL. An ATP stock solution was also prepared at a concentration of 50 mM. ATP solution was added into different polycation solutions to obtain different final concentrations of ATP (0, 0.1, 0.2, 0.4, 1, 2, 4, 5 mM), followed by zeta potential measurement.

### Colloidal stability and serum stability

To evaluate the colloidal stability of the crosslinked polyplex, the polyplex was incubated at 4

°C and the particle size was monitored at time intervals by DLS.

For serum stability, polyplex was incubated in 10% FBS at 37 °C and the particle size was measured at different times. The replacement of siRNA by serum was also checked by agarose gel electrophoresis.

### Cytotoxicity analysis and hemolysis assay

The cytotoxicity of different polycations (25k PEI, 1.8k PEI, PEI-PBA and CrossPPA) was measured by MTT assay. Briefly, the cell lines were incubated with increasing concentrations of the polymers for 24 h. Then, the MTT reagent (5 mg/mL in PBS) was added and the cells were incubated for an additional 4 h. The solutions contained MTT were carefully removed and DMSO was added to dissolve formazan, followed by measurement of the absorbance at 570 nm.

The cytotoxicity of polyplex was also evaluated. The polyplexes composed of siNC and 25k PEI, 1.8k PEI, PEI-PBA and CrossPPA were prepared at various w/w ratios and then diluted with FBS-free medium at a siNC concentration of 100 nM. After incubation with cells for 4 h, the old medium was replaced with 10% FBS-containing medium for another 20 h. The MTT assay was performed as described above.

For hemolysis assay, red blood cells (RBCs) were obtained from healthy rats and diluted with PBS (pH 7.4) at 2% concentration. Different polyplexes (w/w 4:1) were diluted with PBS (pH 7.4) to 1 mg/mL of PEI, then incubated with RBC solution at 37 °C for 2 h; water treatment was set as positive control and PBS as negative control. After incubation, the mixtures were centrifuged at 8000 rpm for 10 min. The supernatants were collected and the absorbance (570 nm) of each sample was detected by Synergy 2 Multifunctional Microplate Reader (BioTek, USA). The percentage of hemolysis was calculated according to the following formula: hemolysis ratio (%) =  $(A_{\text{sample}} - A_{\text{negative}}) / (A_{\text{positive}} - A_{\text{negative}}) \times 100\%$ .

### Cell uptake and endosomal escape

4T1 cells were seeded into 24-well plates and cultured for 24 h. The next day, cells were treated with Free FAM-siRNA, 1.8k PEI/FAM-siRNA, PEI-PBA/FAM-siRNA or CrossPPA/FAM-siRNA (FAM-siRNA 1.33 µg/mL, w/w 4:1, diluted with RPMI-1640 medium) for 2 h. To block the sialic acid, 4T1 cells were pretreated with 50 mM free PBA for 30 min. After incubation, the cells were washed and collected, then detected by flow cytometry (BD FACSCalibur).

For the observation of endo/lysosomal escape, 4T1 cell lines were seeded in confocal microscopy dishes and cultured for 24 h at 37 °C, followed by incubation with 1.8k PEI/FAM-siRNA, 1.8k

PEI-PBA/siRNA and CrossPPA/FAM-siRNA polyplex (FAM-siRNA 1.33  $\mu\text{g}/\text{mL}$ , w/w 4:1, diluted with RPMI-1640 medium) for 3 h. Afterwards, the cells were washed with PBS twice and incubated with fresh medium for 0 and 3 h, followed by washing with PBS thrice and incubating with LysoTracker Red for 40 min at 37 °C. The cells were then washed with PBS twice and immediately observed using a confocal laser scanning microscope (Carl Zeiss LSM 700, Germany).

### Intracellular ATP-dependent siRNA release

To verify the intracellular ATP-dependent siRNA release, low temperature (4 °C) and iodoacetic acid (IAA) at 37 °C were used to inhibit ATP production in the cells. 4T1 cells were seeded in confocal microscopy dishes at a density of  $1 \times 10^5$  cells per well. After culturing for 24 h, the cells were incubated with cy3-/cy5-siRNA coloaded CrossPPA polyplex (both cy3-siRNA and cy5-siRNA were 100 nM, polymer/siRNA w/w = 4:1) at 37 °C for 4 h and then washed by PBS twice, following by incubation with medium (37 °C), low temperature and iodoacetic acid (IAA) for an additional 4 h. Subsequently, the 4T1 cells were washed by PBS twice and observed *via* CLSM. The observation parameters of CLSM were Cy3  $\lambda$  ex/em = 550/570 nm, Cy5  $\lambda$  ex/em = 550/670 nm.

### Luciferase silencing *in vitro*

Luciferase silencing assay was performed on 4T1-Luc cell lines, which stably express luciferase. 4T1-Luc cells were seeded in 48-well plates at a density of  $1 \times 10^4$  cells per well. After culturing for 24 h, luciferase-specific siRNA (siLuc) polyplexes (25k PEI/siLuc, 1.8k PEI/siLuc, PEI-PBA/siLuc and CrossPPA/siLuc) diluted with FBS-free or 10% FBS-containing medium were added and incubated for 4 h, followed by replacement with fresh medium for an additional 20 h. Then, the luciferase activity was measured by a microplate reader (BioTek Synergy2, America) using a luciferase assay kit (Beyotime, China).

### Downregulation of Bcl2 protein, cell growth inhibition and cell apoptosis assay

4T1 cells were seeded in 12-well plates at a density of  $1 \times 10^5$  cells per well. The next day, the cells were treated with PBS, Free siBcl2, 25k PEI/siBcl2, 1.8k PEI/siBcl2, PEI-PBA/siBcl2 and CrossPPA/siBcl2 at an siBcl2 concentration of 100 nM for 4 h, followed by incubation with medium for an additional 40 h. After that, protein of each group was collected and Bcl2 protein expression was detected by Western Blot. Cell growth inhibition was measured by MTT assay. Briefly, 4T1 cells ( $5 \times 10^3$  cells per well)

were seeded in 96-well plates. The next day, the same treatment as in the Bcl2 silencing assay was performed. After incubation, cell viability was detected by MTT assay.

For cell apoptosis assay, the cells ( $1 \times 10^5$  cells per well) were seeded in 12-well plates. After incubation for 24 h, the cells were transfected with siBcl2 by the same method mentioned in the cell growth inhibition experiment and were detected using the Annexin V-FITC Apoptosis Detection Kit by flow cytometry (BD FACSCalibur).

### Animals and tumor model

A 4T1 tumor model was established by subcutaneous injection of 4T1 cells ( $1 \times 10^6$ ) into selected positions. The tumor size was monitored by a vernier caliper, and the tumor volume (V) was calculated as  $V = L \times W^2 / 2$ , where L and W are the length and width of the tumor, respectively.

### Pharmacokinetics study

The SD rats were randomly divided into 4 groups: Free FAM-siRNA, 1.8k PEI/FAM-siRNA, 1.8k PEI-PBA/siRNA and CrossPPA/FAM-siRNA. The mice were intravenously injected with different formulations (FAM-siRNA, 0.15 mg/kg). The blood samples were collected at time intervals and centrifuged at  $10,000 \times g$  for 15 min. The fluorescence intensity of FAM-siRNA in the plasma was measured by Synergy 2 Multifunctional Microplate Reader (BioTek, USA).

### *In vivo* biodistribution

For *in vivo* biodistribution study, the mice were divided randomly into 3 groups (n=3). Cy5-labeled siRNA was loaded into the polyplexes for indicating the siRNA distribution. Mice were administrated with 1.8k PEI/cy5-siRNA, 1.8k PEI-PBA/cy5-siRNA and CrossPPA/cy5-siRNA polyplexes separately by *i.v.* injection. Caliper IVIS Lumina II *in vivo* image system was utilized to monitor the distribution behavior of the polyplexes and images were obtained at 6 h, 12 h, 24 h after injection. After 24 h, the tumors and main organs were harvested from the mice, followed by fluorescence imaging.

### *In vivo* anti-tumor study

The tumor-bearing mice were weighed and randomly divided into different groups (n=6) when the tumor volume reached 60 mm<sup>3</sup>, and treated with 150  $\mu\text{L}$  of physiological saline, CrossPPA/siNC, 1.8k PEI/siBcl2, PEI-PBA/siBcl2 and CrossPPA/siBcl2 polyplexes on every 4 days intravenously. All polyplexes contained 20  $\mu\text{g}$  siRNA/mice per injection. The tumor size and body weight of the mice were recorded every other day. After 20 days, the tumor

was harvested and Bcl2 level of each tumor was analyzed by Western blot. Additionally, H&E staining and TUNEL analysis were also performed on tumor sections.

### Statistical analysis

All quantitative data are expressed as mean  $\pm$  S.D. unless otherwise noted. Data were analyzed using two-tailed Student's *t*-test for 2 groups. Probabilities less than 0.05 were considered significant.

## Results and Discussion

### Synthesis and characterization of PEI-PBA

The synthesis procedure of PEI-PBA is shown in **Figure S1**. Briefly, the carboxyl group of 4-carboxyphenylboronic acid was activated by EDC and reacted with the amine group of PEI. After reaction, the product was dialyzed against distilled water for 48 h to remove unreacted EDC and PBA. The structure of PEI-PBA was validated by <sup>1</sup>H-NMR, <sup>13</sup>C-NMR and FTIR. As shown in **Figure S2A**, phenyl proton signals of 4-carboxyphenylboronic acid groups occurred at 7.6–7.2 ppm and the ethylene proton signals of PEI was present at 3.0–2.0 ppm. The substitution degree of PBA to PEI was 20.6% as calculated from the peak integrations. **Figure S2B** exhibits the <sup>13</sup>C-NMR result. The peak between 120–140 ppm was the signal of benzene on PBA. The characteristic IR absorption bands (**Figure S2C**) at 1369.4 cm<sup>-1</sup> were attributed to B-O stretching, whereas the bands at 1545.9 cm<sup>-1</sup> (C-O stretching) and 1533.4 cm<sup>-1</sup> (–NH–CO– stretching) were the characteristic absorbances of the amide group of PEI-PBA [29]. Hence, the <sup>1</sup>H NMR and FTIR spectra confirmed the conjugation of PBA to PEI.

### Characterization of polyplex

The PEI-PBA/alginate w/w ratio was optimized by the luciferase silencing efficiency of CrossPPA/siLuc on 4T1 cells. As shown in **Figure S3**, w/w 10:1 showed the best performance. Therefore, 10:1 of PEI-PBA/alginate was chosen for further research. Particle size and zeta potential of the polyplexes were measured by dynamic light scattering (DLS) at w/w ratios of 1, 2 and 4. As shown in **Figure 1A–B**, the size decreased with the increase in w/w ratio, which could be ascribed to enhanced binding of the polycation and siRNA. Furthermore, both PBA modification and alginate crosslinking decreased the particle size. The zeta potential was enhanced with increased w/w ratio. PEI-PBA showed a higher zeta potential than PEI, which was attributed to the hydrophobicity of PBA. The modification of hydrophobic moieties on PEI promoted the formation

of nanoparticles and the condensed surface zeta potential [30]. However, it decreased after crosslinking with alginate, which was attributed to the anionic property of alginate.

siRNA encapsulation was determined by agarose gel electrophoresis (**Figure 1C**). The effects of PBA modification and crosslinking on both polyplexes formation and siRNA loading were evaluated by electrophoresis. The result indicated that 25k PEI shows superior siRNA encapsulation ability than 1.8k PEI because of its higher molecular weight. Meanwhile, CrossPPA exhibited good siRNA loading ability, which was similar to that of 25k PEI. The crosslinking between PEI-PBA and alginate was thought to form a higher MW polycation and improve siRNA encapsulation consequently.

### ATP-triggered release of siRNA

PBA can reversibly bind to different diols [31]. The CrossPPA polycation formed based on chemical binding between PBA of the PEI-PBA and diols on the alginate. Additionally, the PBA could also bind with the sugar end group of siRNA. When the cross-linked polyplex reaches a diol-rich environment, the original structure could be dissociated by forming new borate ester bonds. Since the intracellular ATP concentration in tumor cells could reach as high as 5 mM [12], much higher than the extracellular concentration, the effect of ATP on the CrossPPA polyplex disassembly was evaluated. As shown in **Figure 2A**, both PEI-PBA and CrossPPA groups showed burst release of siRNA from polyplexes with the treatment of 5 mM ATP. The release of siRNA from polyplexes treated with different concentrations of ATP was also monitored at time intervals. As shown in **Figure 2B**, within 120 min, relatively no siRNA released from 25k PEI/siRNA or 1.8k PEI/siRNA even when the ATP concentration was as high as 5 mM. In contrast, PEI-PBA/siRNA and CrossPPA/siRNA released almost all of their siRNA within 5 min, indicating the burst release behavior. Furthermore, when PEI-PBA/siRNA and CrossPPA/siRNA were treated with 1 mM ATP, 60% siRNA released from the polyplexes within 60 min. These results demonstrated that the release of siRNA from PEI-PBA/siRNA and CrossPPA/siRNA was time and ATP concentration dependent. The burst release of siRNA from CrossPPA/siRNA could be ascribed to the decrosslinking of PEI-PBA-alginate and PEI-PBA-siRNA or charge reversal of PEI-PBA.

We hypothesized that both diol and phosphate play important roles in the release of siRNA. Therefore, the detailed release mechanism was further studied to know the effects of diol and phosphate in siRNA release and the probable procedure of that. We

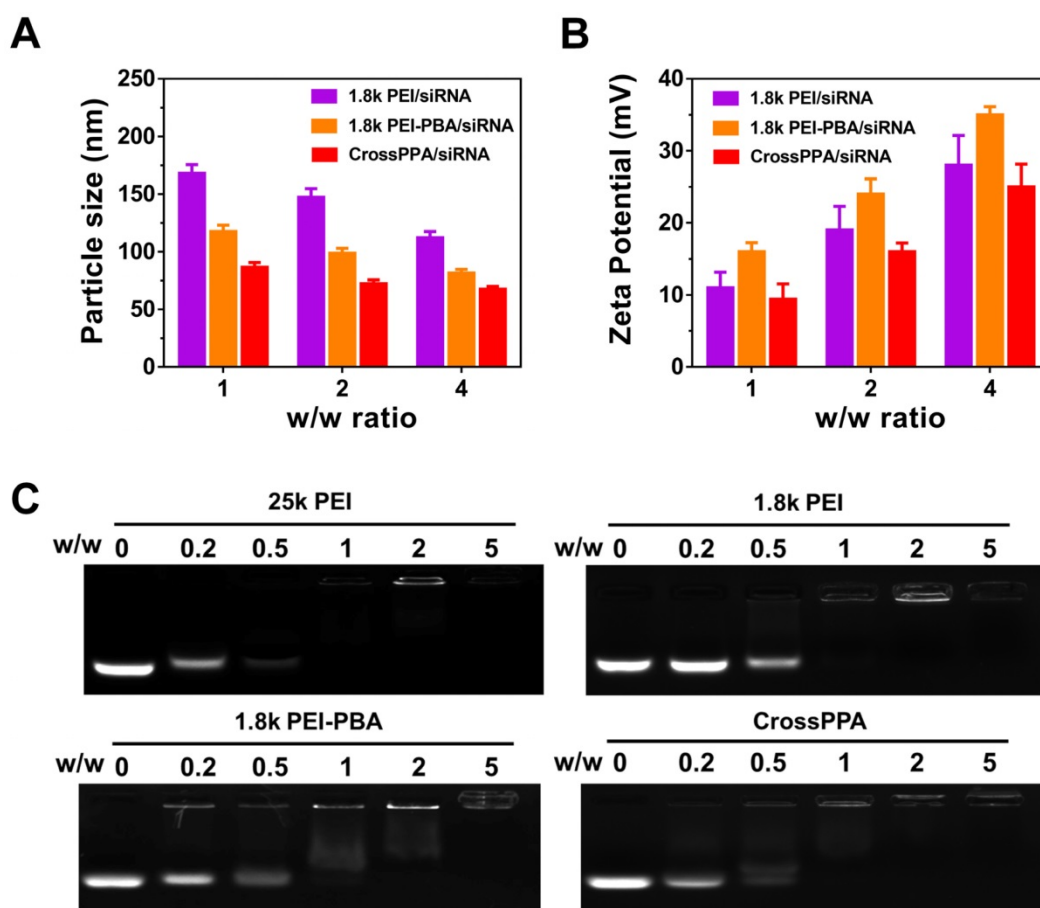


**Figure 1.** Polyplexes formation and characterization. **(A)** Particle size and **(B)**  $\zeta$  potential of 1.8k PEI, PEI-PBA/siRNA, CrossPPA/siRNA polyplexes prepared at different w/w ratios. The w/w ratios of 1, 2, and 4 were equal to N/P of 7.4, 14.8, and 22.2. **(C)** siRNA encapsulation assessed by agarose gel electrophoresis of polyplexes prepared at different w/w ratios. The w/w ratios of 0, 0.2, 0.5, 1, 2, and 5 were equal to N/P of 0, 1.48, 3.7, 7.4, 14.8, and 22.2.

proposed the following release mechanism (**Scheme 1**): ATP competed for binding with PBA and replaced alginate and siRNA, leading to decrosslinking of CrossPPA and PBA-siRNA. Next, the negatively charged ATP reversed PEI-PBA's positive charge, resulting in release of negatively charged siRNA from the carrier because of electrostatic repulsion.

The importance of ATP binding to PBA and the ATP negative charge for siRNA release was verified by adenosine and dATP incubation. Adenosine was used as an uncharged trigger and dATP was used as a diol-free trigger. As indicated in **Figure 3A**, for the PEI-PBA/siRNA group, uncharged adenosine could not trigger the release of siRNA, which proved the importance of the negative charge on ATP. In addition, diol-free dATP showed only a weak siRNA release, indicating that electrostatic competition alone was not able to trigger the release of siRNA. Thus, we can conclude that the dynamic chemical binding between PBA and ATP was the requirement for siRNA release from PBA-modified polycation. The CrossPPA polyplex showed a similar result as PEI-PBA/siRNA with dATP treatment, while it showed a different result under uncharged adenosine

treatment. Some siRNA released from the crosslinked polyplex due to disassembly of the crosslinks with diol moiety treatment. Adenosine could destabilize the CrossPPA crosslinking and weaken the siRNA affinity to the carrier, leading to the release of siRNA. The result indicated that diol in ATP acted as the precondition and negative charge as the key factor for accelerated release of siRNA from CrossPPA/siRNA polyplex.

Phosphate and glucose in the blood could also affect the stability of polyplexes. To evaluate the selectivity of PEI-PBA and CrossPPA to intracellular ATP, their stability in phosphate and glucose was also studied. As shown in **Figure S4**, no siRNA release was found from the 25k PEI/siRNA group after incubation with phosphate and glucose. However, obvious leakage of siRNA was detected in the 1.8k PEI/siRNA group, which was probably because of the weak binding of 1.8k PEI with siRNA. Interestingly, PEI-PBA/siRNA and CrossPPA/siRNA maintained their stability and avoided being destroyed by phosphate and glucose, proving their selective responsive to ATP.

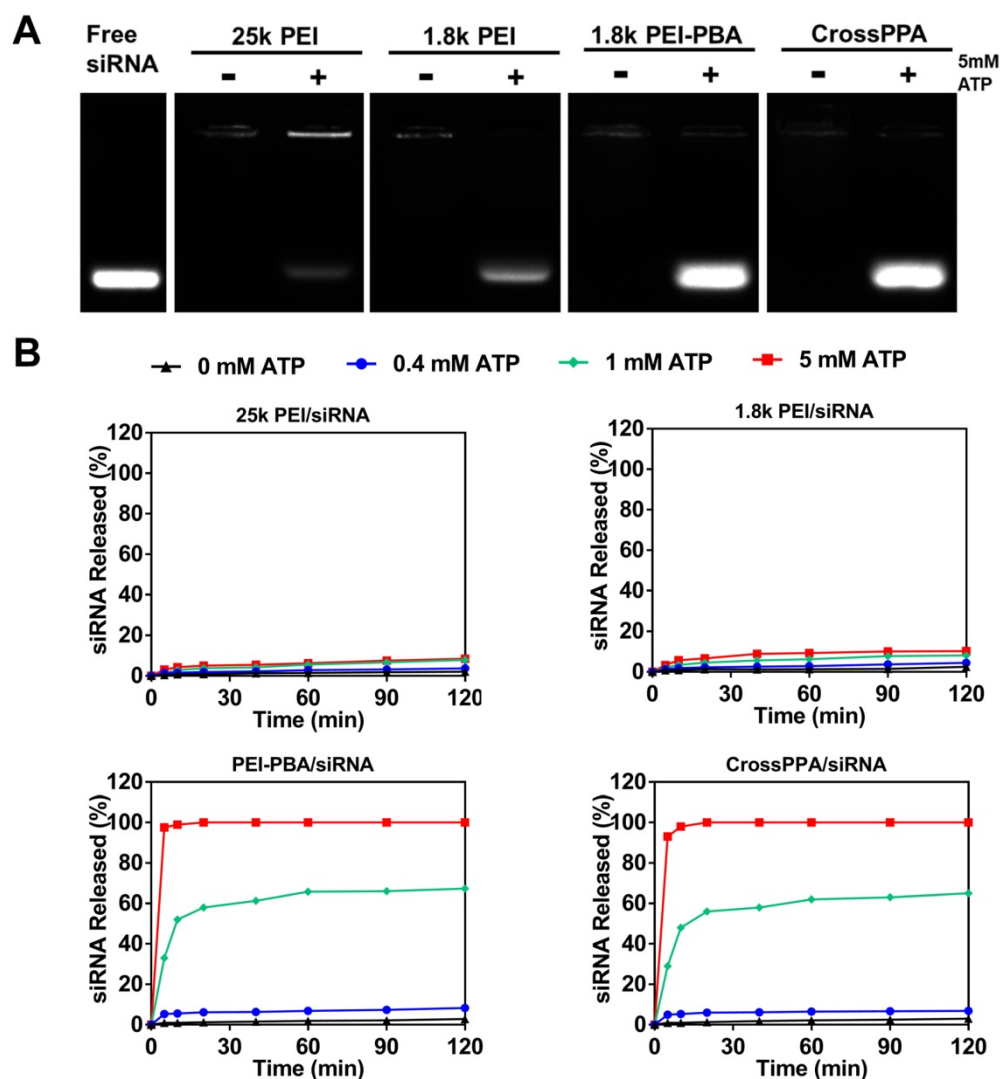


**Figure 2.** (A) ATP-triggered release of siRNA from different polyplexes, where the detection was performed immediately after mixing ATP with polyplexes. (B) siRNA release study of 25k PEI/siRNA, 1.8k PEI/siRNA, PEI-PBA/siRNA and CrossPPA/siRNA triggered with 0, 0.4, 1, and 5 mM ATP separately and monitored at time intervals.

Morphological observation was also performed on CrossPPA/siRNA polyplex before and after ATP treatment. After treatment with 5 mM ATP, the particle size increased to around 900 nm and the structure of the polyplex became loose and diffuse (**Figure 3B**). The added ATP could effectively react with PBA and force the disassembly of the crosslinks, making the structure become loose. In addition, the absorbed ATP moieties on PEI-PBA could interact with other PEI-PBA chains, which would promote aggregation of PEI-PBA-ATP, as indicated by the larger particle size.

From the data shown above, we hypothesized that PEI-PBA and CrossPPA accelerated charge reversal under ATP treatment. ATP was added to PEI-PBA and CrossPPA solutions to obtain environments with different concentrations of ATP. At higher ATP concentration, the zeta potentials of PEI-PBA and CrossPPA decreased sharply while 25k

PEI and 1.8k PEI decreased smoothly (**Figure 3C**). Furthermore, the zeta potentials of PEI-PBA and CrossPPA reversed from positive to negative when the ATP concentration was higher than 1 mM. Thus, PBA modification was proved to make the cationic polymer more sensitive to ATP and achieve faster charge reversal compared with unmodified polymer, which was due to the violent reaction between PBA and ATP, forcing enrichment of ATP in the polyplex (**Figure 3D**). We also measured the charge reversal of polyplexes after incubation with ATP. As shown in **Figure S5**, the zeta potential of both 25k PEI/siRNA and 1.8k PEI/siRNA decreased smoothly after ATP was added, indicating that binding of ATP with the polyplex was difficult. However, 1.8k PEI-PBA and CrossPPA polyplexes showed sharp decreases and even reversal of their zeta potentials. This validated that ATP could effectively trigger the charge reversal of PEI-PBA, CrossPPA and their polyplexes.

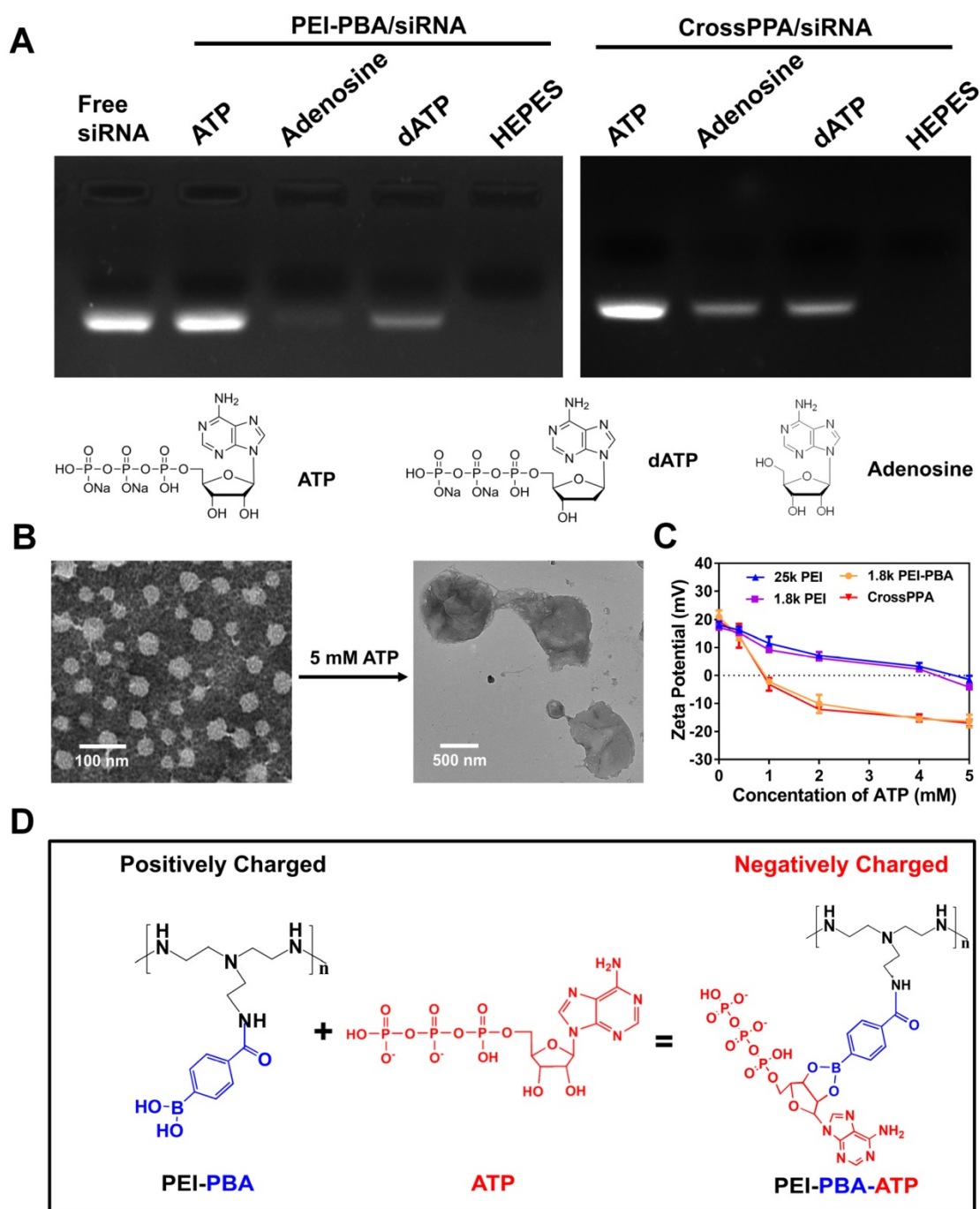


**Figure 3.** (A) Release mechanism studied by treatment with ATP, dATP and adenosine. (B) Morphological observation of CrossPPA/siRNA polyplex before and after 5 mM ATP treatment. (C) Charge reversal of 25k PEI, 1.8k PEI, PEI-PBA and CrossPPA with different amounts of ATP added. (D) Reaction scheme of the charge reversal of PEI-PBA with treatment of ATP.

### Colloidal stability and serum stability

The CrossPPA/siRNA polyplex exhibited good colloidal stability and the particle size showed no significant change after 2 days (Figure S6A). For *in vivo* application of cationic polyplexes, serum stability is of great importance because cationic polyplexes tend to aggregate or disassemble in serum due to nonspecific protein absorption and RNase degradation. Here, we studied serum stability by

measuring the particle size by DLS and siRNA protection by agarose gel electrophoresis. For particle size measurement, CrossPPA/siRNA polyplex was incubated with rat serum for different times, followed by DLS size detection. As shown in Figure S6A, the particle size showed no significant change after serum treatment. We further investigated the protective effect of CrossPPA on siRNA from RNase degradation in the serum. The agarose gel electrophoresis results indicated that most of the

siRNA was still intact, without being degraded by RNase in the serum even after 24 h (Figure S6B).

### Cytotoxicity

The cytotoxicity of a siRNA delivery vector plays a crucial role for transfection and therapy applications. Low molecular weight PEI was thought to alleviate the toxicity on cells because it is easier to be metabolized by the cells [32]. Here, we studied the toxicity of 25k PEI, 1.8k PEI, 1.8k PEI-PBA and CrossPPA in 4T1 cell lines. The 25k PEI was so toxic to

cells that the cell viability was lower than 50% when the concentration was around only 20  $\mu\text{g}/\text{mL}$  (Figure 4A). It was shown that 1.8k PEI, 1.8k PEI-PBA and CrossPPA displayed much lower cytotoxicity than 25k PEI. The cell viabilities were still higher than 50% when the PEI concentration reached 100  $\mu\text{g}/\text{mL}$  with 1.8k PEI, 1.8k PEI-PBA and CrossPPA. The result may be ascribed to the low molecular weight of 1.8k PEI and 1.8k PEI-PBA and ATP-triggered degradation of CrossPPA.

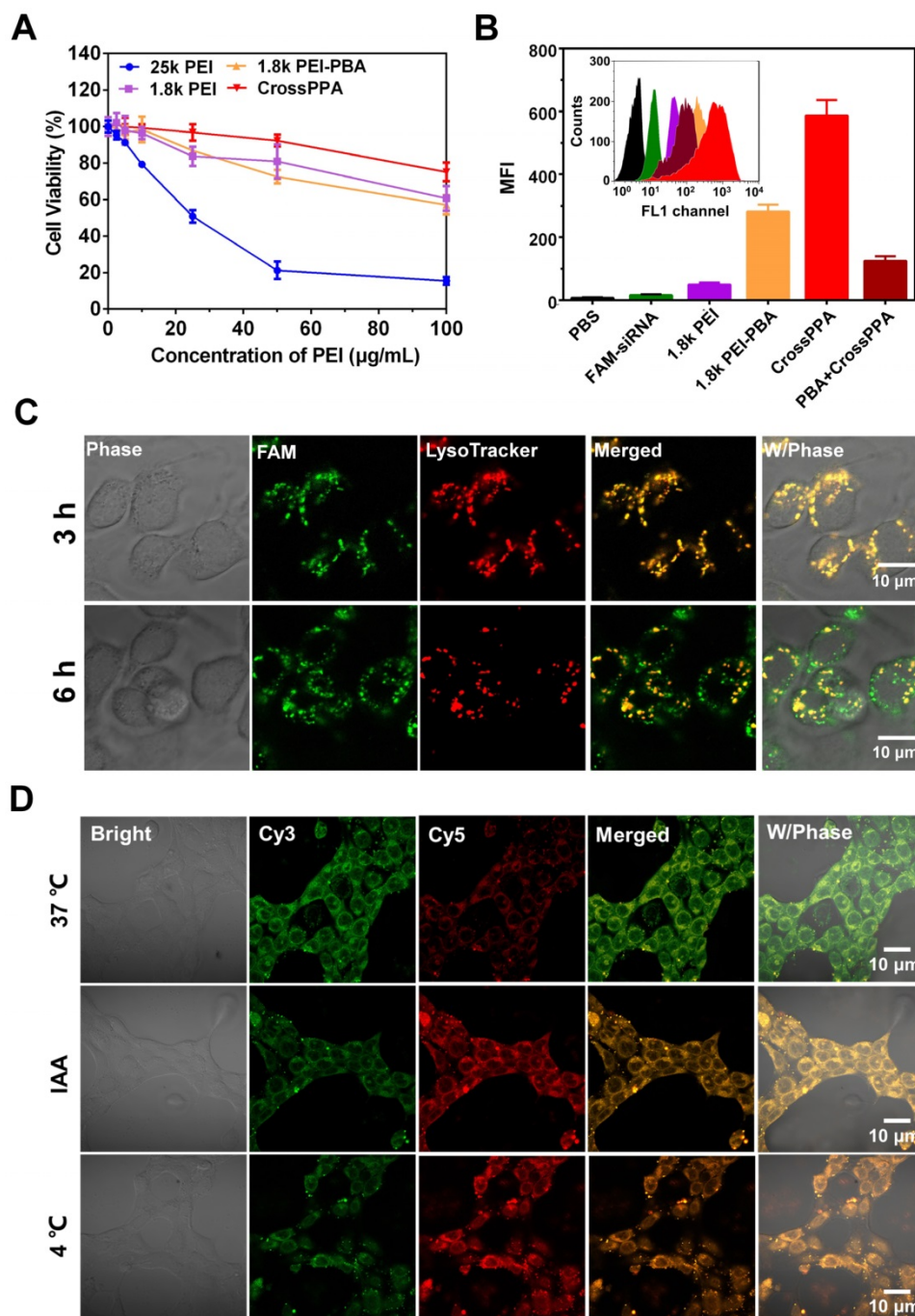


**Figure 4.** (A) Cytotoxicity of polycations 25k PEI, 1.8k PEI, PEI-PBA and CrossPPA by MTT assay. (B) Cell uptake analysis of various FAM-siRNA-loaded polyplexes at w/w=4. (C) Endosomal escape of polyplexes in 4T1 cells 3 and 6 h after incubation. (D) Intracellular ATP-triggered siRNA release. 4T1 cells were treated with CrossPPA/cy3- and cy5-siRNA polyplex and observed by CLSM, incubating at 37 °C, 4 °C, and with the ATP inhibitor iodoacetic acid (IAA) at 37 °C.

We further studied the safe w/w ratios of polyplexes on 4T1 cells using MTT assay. As shown in **Figure S7A**, there was no significant cytotoxicity on 4T1 cell lines when the w/w ratios were 1, 2, or 4. Therefore, these w/w ratios were chosen for the following experiments.

The hemolysis properties of the polyplexes were evaluated by incubation with red blood cells. As shown in the result, 25k PEI/siRNA caused 22% hemolysis compared with the water treatment group, which was because of the strong positive charge and difficult degradation of 25k PEI. Interestingly, the other groups based on 1.8k PEI/siRNA didn't cause remarkable hemolysis, indicating the safe application of 1.8k PEI-based polyplexes.

### Cell uptake mediated by SA

PBA is reported as a potential tumor-targeting ligand because it has affinity to sialic acid (SA), which is overexpressed on many tumor cells [26, 27]. 4T1 cells were reported to overexpress SA [33, 34]. The crosslinking of PBA with alginate may affect the binding of PBA with SA [35]. Therefore, the tumor-targeting ability of the crosslinked polyplex was investigated by flow cytometry. Interestingly, the result in **Figure 4B** shows that the cell uptake of CrossPPA/FAM-siNC was better than PEI-PBA/FAM-siNC. In addition, the cell uptake decreased sharply when the cells were pretreated with free PBA, which was used to compete for binding to the SA receptor with crosslinked polyplex. The enhanced targeting ability might be ascribed to the enriched PBA distribution on the tight nanostructure of the crosslinked polyplex. Therefore, it can be concluded that the crosslinking of PBA with alginate did not affect the SA targeting ability of PEI-PBA; instead it enhanced the cell uptake of the polyplexes.

### Endosomal/lysosomal escape

After internalization of the polyplexes, endo/lysosomal escape is a key step for successful transfection and gene silencing. Here, endo/lysosomes and siRNA were separately labeled with red and green fluorescence dyes. The co-localization or separation of endo/lysosome and siRNA was used to check endo/lysosomal entrapment or escape. As shown in **Figure S8**, the fluorescence signal of FAM-siRNA was weak in 1.8k PEI/siRNA-treated cells. After the cells were incubated with 1.8k PEI-PBA/siRNA for 3 h, strong overlap of the green signal with the red signal was observed, meaning trapping of the polyplex in lyso/endosomes. When the cells were incubated for an additional 3 h, obvious separation of green signal from red signal was found, which meant successful

endo/lysosomal escape of PEI-PBA/siRNA polyplex. CrossPPA/siRNA polyplex showed a similar result as PEI-PBA/siRNA. After cells were incubated with CrossPPA/FAM-siRNA for 3 h, the green fluorescence of FAM-siRNA was found to be co-localization with the red signal of LysoTracker (**Figure 4C**). However, some separated fluorescence signals of FAM-siRNA and LysoTracker were clearly observed after 6 h incubation, implying efficient endo/lysosomal escape of the complex. This result indicated that the loaded siRNA could be effectively delivered to the cytosol and therefore perform RNAi. The successful endosomal escape was due to the proton sponge effect of PEI in the polyplexes, promoting endosomal rupture.

### Intracellular ATP-triggered siRNA release from CrossPPA polyplex

Intracellular ATP-triggered siRNA release was validated by fluorescence resonance energy transfer (FRET). siRNAs labeled with the donor dye cy3 (green) and the acceptor dye cy5 (red) were co-encapsulated within the polyplex (FRET polyplex). When the FRET dyes were co-loaded in the polyplex, the energy of cy3 transferred to cy5, generating strong cy5 fluorescence. Correspondingly, the fluorescence of cy5 decreases after siRNA is released due the increased dye separation distance. 4T1 cell lines were incubated for 4 h with FRET polyplex, then incubated with fresh medium for an additional 4 h in different conditions [28]. For building a low intracellular ATP concentration model [13], 4T1 cells were incubated at low temperature (4 °C) or in the presence of iodoacetic acid (IAA) at 37 °C, which was reported to inhibit ATP generation. As shown in **Figure 4D**, cells showed strong cy3 fluorescence signal and low cy5 signal, which indicated successful disassembly of the polyplex in the cells incubated at 37 °C. However, the low temperature and IAA-treated groups showed high cy5 signal, indicating strong FRET between cy3 and cy5 and intact structure of the polyplex in the cells. Hence, the release of siRNA in the cytosol was validated to be triggered by ATP.

### Transfection and silencing of luciferase

The transfection ability and silencing of luciferase were determined using a luciferase kit. The safe w/w ratios of 1.8k PEI, PEI-PBA and CrossPPA for transfection were chosen as 1, 2, and 4. As shown in **Figure 5A**, 1.8k PEI showed low luciferase silencing efficiency due to its low charge density [36]. Only 15% luciferase was silenced even when the w/w reached 4 for the 1.8k PEI group. As has been reported, PEI-PBA itself has higher gene transfection ability than 1.8 k PEI owing to its hydrophobic moiety and targeting

ability [29]. However, up to now, there has been no paper mentioning the siRNA release mechanism from PEI-PBA polyplex. As is known to us, burst release of siRNA from the carrier in the cytosol plays a crucial role in gene delivery and successful gene silencing.

In this study, we found that the high transfection efficiency of PEI-PBA could also be ascribed to the fast release of siRNA in the cells triggered by ATP. The result shown in **Figure 5A** agrees well with a previous report [29]. Most important, crosslinking with alginate further improved the transfection efficiency, owing to the improved uptake, ATP-triggered disassembly and rapid siRNA release in the cytosol. The polyplex achieved 75% luciferase silencing efficiency at w/w=4, which was significantly different from PEI-PBA. In addition, the crosslinked polymer exhibited better performance than the positive control 25k PEI, which only silenced 50% luciferase at w/w=2. All of these results demonstrated that both the PBA modification and crosslinking with alginate were beneficial for siRNA delivery and gene silencing. Next, cell transfection was performed in 10% FBS-containing medium. As shown in **Figure S9**,

CrossPPA/siRNA showed an obvious advantage for siLuc transfection.

### Tumor cell killing, Bcl2 silencing and cell apoptosis

The crosslinked polymer exhibited good performance for luciferase silencing. We next studied the therapeutic potential of CrossPPA for tumor therapy. Bcl2, an anti-apoptosis factor in malignant cells, has been reported to be a key factor for tumor survival [37]. The successful transfection of siRNA targeting Bcl2 can downregulate Bcl2 expression and induce cell apoptosis. Hence, we took Bcl2 as our target therapeutic protein for an anti-tumor study. 4T1 cell lines were incubated with different polyplexes (25k PEI, 1.8k PEI, 1.8k PEI-PBA, CrossPPA) for 4 h and incubated with fresh medium for another 44 h, followed by MTT assay, protein extraction and analysis by western blot. As shown in **Figure 5B**, CrossPPA/siBcl2 effectively killed the tumor cells and the cell viability of the CrossPPA/siBcl2 treatment group was only 43%.

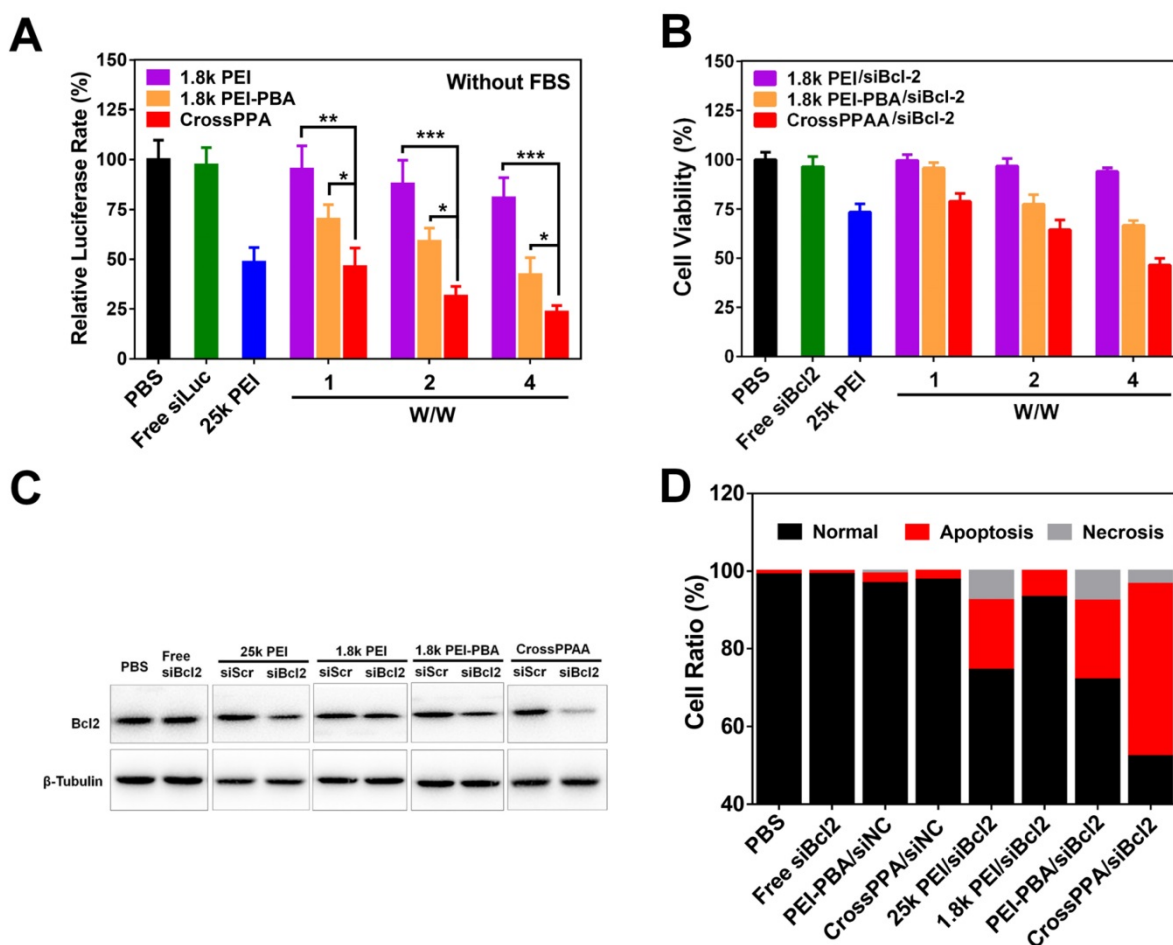


**Figure 5.** (A) Luciferase gene silencing mediated by siLuc-loaded polyplexes at various w/w ratios. \*p < 0.05, \*\*p < 0.01, \*\*\*p < 0.001. (B) 4T1 tumor cell killing of siBcl2-loaded polyplexes. (C) Bcl2 protein expression level after treatment with siBcl2-loaded polyplexes and analysis by western blot. (D) Cell apoptosis analysis by Annexin V-FITC/PI double staining.

The cell killing was attributed to Bcl2 protein silencing. CrossPPA/siBcl2 significantly downregulated the expression of Bcl2 protein in 4T1 cells, while CrossPPA/siScr didn't have any effect on Bcl2 expression (**Figure 5C**). This silencing was thought to be specific to Bcl2 mediated by siBcl2. The silencing efficiency of PEI-PBA/siBcl2 was weaker than that of the CrossPPA group.

Next, cell apoptosis after treatment by different siBcl2-loaded polyplexes was measured by flow cytometry. After the same treatment as siBcl2 transfection, 4T1 cells were double-stained with FITC-Annexin V and PI. Statistical analysis results are shown in **Figure 5D**. The gold standard 25k PEI/siBcl2 induced 17% cell apoptosis, while the low molecular weight 1.8k PEI/siBcl2 only caused 6% apoptosis. Both PEI-PBA/siBcl2 and CrossPPA/siBcl2 exhibited forceful apoptosis induction effects, which were 20% and 43%, respectively. siBcl2-loaded PEI-PBA and CrossPPA polyplexes significantly induced cell apoptosis and therefore killed the tumor cells.

### Pharmacokinetics study

The pharmacokinetics of the polyplexes were evaluated by intravenous injection of FAM-labeled siRNA-loaded polyplexes into rats. As shown in **Figure S10**, the circulation half-life ( $t_{1/2}$ ) of CrossPPA/siRNA is around 2.3 h, much longer than that of free siRNA at 24 min. Additionally, the  $t_{1/2}$  of 1.8k PEI/siRNA and PEI-PBA/siRNA were 38 min and 1.2 h, respectively. The crosslinking strategy was proved to prolong the  $t_{1/2}$  of siRNA and showed better performance than the unmodified PEI or PEI-PBA.

### In vivo biodistribution

To compare the tumor targeting properties of 1.8k PEI, PEI-PBA and CrossPPA polyplexes, real-time *in vivo* fluorescence imaging was used to detect the biodistribution of cy5-siRNA-loaded polyplexes. The modification of PBA on low molecular weight PEI significantly increased the accumulation of cy5-siRNA at the tumor site (**Figure 6A**). 6 h after *i.v.* injection there was no fluorescence of cy5 at the tumor site in the 1.8k PEI/cy5-siRNA group. However, the PEI-PBA and CrossPPA groups showed clear cy5 signal, which could be ascribed to the active targeting property of the PBA-modified polyplexes. Furthermore, the signal intensity remained strong at 24 h post-injection, revealing that PEI-PBA and CrossPPA polyplexes accumulated effectively in the tumor and the latter showed better performance. The tumor accumulation of CrossPPA/siRNA was obtained by EPR (enhanced

permeability and retention)-mediated passive targeting and PBA-mediated active targeting. The particle size of CrossPPA/siRNA was 75 nm at w/w=4, which is suitable for the EPR effect [38]. The PBA-SA interaction promoted the binding of CrossPPA/siRNA polyplex to tumor cells and receptor-mediated endocytosis. After 24 h, mice were sacrificed and the tumor and main organs were fluorescently imaged. As depicted in **Figure S11A**, 1.8k PEI was mainly distributed in the liver and kidney, while PEI-PBA and CrossPPA polyplexes were mainly at the tumor site. Fluorescence quantitative analysis results are also shown in **Figure S11B**. The crosslinking strategy enhanced siRNA accumulation at the tumor site.

### In vivo anti-tumor therapy

The *in vivo* biodistribution result proved the tumor accumulation of PEI-PBA and CrossPPA polyplexes. The anti-tumor efficacy was studied by loading siBcl2 into the polyplexes and using 4T1 tumor-bearing mice. As depicted in **Figure 6B**, the tumors grew rapidly in the CrossPPA/siNC group, showing no significant difference from the saline group and indicating no therapeutic effect of the polymers. In addition, 1.8k PEI/siBcl2 only exhibited a weak anti-tumor effect, which was probably because of its low tumor accumulation and low transfection efficiency in the 4T1 cell line. The PBA-modified PEI polyplex inhibited tumor growth significantly owing to its obvious tumor targeting and high transfection efficiency. Most important, it is worth noting that the crosslinked polyplex (CrossPPA/siBcl2) exhibited superior anti-tumor efficacy compared with PEI-PBA/siBcl2. The outstanding performance of the crosslinked polyplex for tumor accumulation and gene transfection finally lead to optimal *in vivo* tumor suppression efficacy. At the end of treatment, the tumors were harvested and weighed (**Figure S12A**) and the tumor inhibition ratio was also calculated (**Figure S12B**). The tumor inhibition ratio of CrossPPA/siBcl2 reached as high as 90%. Representative *ex vivo* images were also taken (**Figure S13**). The tumor size and tumor weight of the CrossPPA/siBcl2 group were much smaller than those of the other groups. Furthermore, the body weights of the mice did not show obvious changes during the period of treatment with each formulation, indicating the low systemic toxicity of the polyplexes (**Figure S14**).

To validate that the 4T1 tumor growth inhibition was due to Bcl2 gene silencing, we used western blotting to analyze the expression of the Bcl2 protein in tumor after different treatments. As shown in **Figure 6C**, there was a clear decrease in the Bcl2

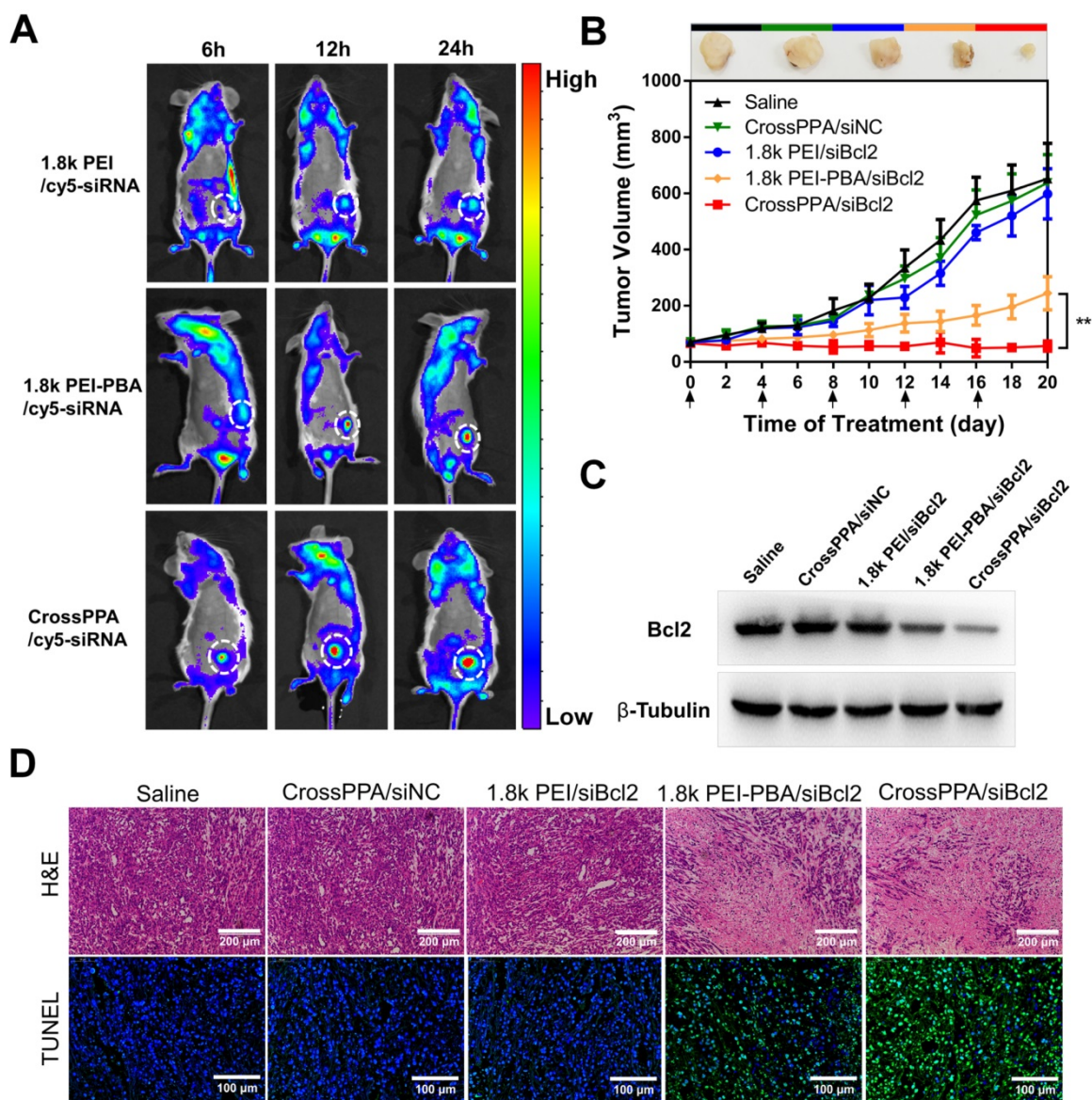


**Figure 6.** (A) Tumor targeting ability of polyplexes assessed by an *in vivo* imaging system. White circles: tumor. (B) 4T1 tumor growth curves of different groups after treatment on the indicated days (shown by arrows). siNC and siBcl2 were administered at a dose of 1.2 mg/kg. Data are shown as mean  $\pm$  SD (n = 6). \*\*p < 0.01. (C) Expression of Bcl2 protein in tumors after different treatments. (D) H&E and TUNEL staining of tumor sections after different treatments.

protein level after treatment by PEI-PBA/siBcl2 and CrossPPA/siBcl2. The expression of Bcl2 after CrossPPA/siBcl2 treatment was only 19.2% (Figure S15) compared with that of the saline group. Additionally, CrossPPA/siNC did not cause any downregulation of Bcl2 protein expression compared to the saline group, confirming the effect of transfected siBcl2 on Bcl2 protein.

H&E and TUNEL staining were performed on tumor sections (Figure 6D). The histological images indicated that after applying CrossPPA/siBcl2, a massive cancer cell apoptosis occurred in the tumor tissue. Moreover, the tumor sections of the CrossPPA/siBcl2 group showed the strongest green fluorescence signal, indicating the highest level of cell apoptosis. The result proved that the superior tumor

growth suppression was due to the significant apoptosis induced by CrossPPA/siBcl2.

Thus, we can conclude that the successful delivery and transfection of siBcl2 finally lead to downregulation of Bcl2 expression and activation of cell apoptosis, which caused obvious tumor suppression.

## Conclusions

In this research, we have reported a novel siRNA delivery system that, for the first time, apply the combined strategy of “degradation” and “charge reversal”. The crosslinked polymer was initially strongly positively charged and effectively packaged siRNA but became de-crosslinked and negatively charged once triggered by intracellular ATP. The

crosslinking improved siRNA loading, cell uptake and tumor accumulation significantly. Additionally, the stimulus-responsive decrosslinking and charge reversal of the carrier achieved controlled release of siRNA in the cell. It increased the gene transfection efficiency obviously and siBcl2-loaded polyplex also showed good performance for inhibiting 4T1 tumor growth. Furthermore, we should note that the biodegradable carrier showed low cytotoxicity and no significant systemic toxicity. Hence, we can conclude that the ATP-activated charge reversal crosslinked polycations hold tremendous potential for application to *in vitro* siRNA transfection, *in vivo* siRNA delivery and tumor therapy.

## Abbreviations

ATP: adenosine triphosphate; dATP: deoxyadenosine triphosphate; CLSM: confocal laser scanning microscope; CrossPPA: crosslinking of phenylboronic acid grafted polyethyleneimine with alginate; cy3-siNC: cyanine3 labeled siNC; cy5-siNC: cyanine5 labeled siNC; DLS: dynamic light scattering; DMSO: dimethyl sulphoxide; EDC.HCl: 1-ethyl-3-(3-dimethylaminopropyl) carbodiimide hydrochloride; EDTA: ethylenediamine tetra acetic acid; FAM-siNC: 5-Carboxyfluorescein labeled siNC; FBS: fetal bovine serum; FRET: fluorescence resonance energy transfer; FTIR: fourier transform infrared spectroscopy; H&E: haematoxylin and eosin; HEPES: 2-[4-(2-hydroxyethyl)-1-piperazinyl] ethanesulfonic acid; IAA: iodoacetic acid; MTT: 3-(4,5-dimethylthiazol-2-yl)-2,5-diphenyltetrazolium bromide; MWCO: molecular weight cut off; NMR: nuclear magnetic resonance; PBA: phenylboronic acid; PBS: phosphate buffer solution; PEI: polyethyleneimine; PEI-PBA: phenylboronic acid grafted polyethyleneimine; RBCs: red blood cells; SA: sialic acid; siBcl2: Bcl2 targeting siRNA; siLuc: luciferase targeting siRNA; siNC: negative control siRNA; siRNA: small interfering RNA; TEM: transmission electron microscope; TUNEL: terminal deoxynucleotidyl transferase dUTP nick end labeling.

## Supplementary Material

Supplementary figures.

<http://www.thno.org/v08p4604s1.pdf>

## Acknowledgements

This work was financially supported by the National Science and Technology Major Project (2017YFA0205400), the National Natural Science Foundation of China (No. 81573377), and the Jiangsu Fund for Distinguished Youth (BK20170028).

## Competing Interests

The authors have declared that no competing interest exists.

## References

- Davis ME, Zuckerman JE, Choi CH, Seligson D, Tolcher A, Alabi CA, et al. Evidence of RNAi in humans from systemically administered siRNA via targeted nanoparticles. *Nature*. 2010; 464: 1067-70.
- Oh YK, Park TG. siRNA delivery systems for cancer treatment. *Adv Drug Deliv Rev*. 2009; 61: 850-62.
- Pecot CV, Calin GA, Coleman RL, Lopez-Berestein G, Sood AK. RNA interference in the clinic: challenges and future directions. *Nat Rev Cancer*. 2011; 11: 59-67.
- Chen G, Wang K, Hu Q, Ding L, Yu F, Zhou Z, et al. Combining fluorination and bioreducibility for improved siRNA polyplex delivery. *ACS Appl Mater Interfaces*. 2017; 9: 4457-66.
- Liu X, Xiang J, Zhu D, Jiang L, Zhou Z, Tang J, et al. Fusogenic reactive oxygen species triggered charge-reversal vector for effective gene delivery. *Adv Mater*. 2016; 28: 1743-52.
- Pollard H, Remy J-S, Loussouarn G, Demolombe S, Behr J-P, Escande D. Polyethylenimine but not cationic lipids promotes transgene delivery to the nucleus in mammalian cells. *J Biol Chem*. 1998; 273: 7507-11.
- Sun M, Wang K, Oupický D. Advances in stimulus-responsive polymeric materials for systemic delivery of nucleic acids. *Adv Healthc Mater*. 2018; 7: 1701070.
- Chen G, Wang K, Wang Y, Wu P, Sun M, Oupický D. Fluorination enhances serum stability of bioreducible poly(amido amine) polyplexes and enables efficient intravenous siRNA delivery. *Adv Healthc Mater*. 2017: 1700978.
- Gribble FM, Loussouarn G, Tucker SJ, Zhao C, Nichols CG, Ashcroft FM. A novel method for measurement of submembrane ATP concentration. *J Biol Chem*. 2000; 275: 30046-9.
- Traut TW. Physiological concentrations of purines and pyrimidines. *Mol Cell Biochem*. 1994; 140: 1.
- Marcel L, Barbara S, Castoldi AF, Simone K, Pierluigi N. Intracellular adenosine triphosphate (ATP) concentration: a switch in the decision between apoptosis and necrosis. *J Exp Med*. 1997; 185: 1481.
- Mo R, Jiang T, DiSanto R, Tai W, Gu Z. ATP-triggered anticancer drug delivery. *Nat Commun*. 2014; 5: 3364.
- Qian C, Chen Y, Zhu S, Yu J, Zhang L, Feng P, et al. ATP-responsive and near-infrared-emissive nanocarriers for anticancer drug delivery and real-time imaging. *Theranostics*. 2016; 6: 1053-64.
- Naito M, Ishii T, Matsumoto A, Miyata K, Miyahara Y, Kataoka K. A phenylboronate-functionalized polyion complex micelle for ATP-triggered release of siRNA. *Angew Chem*. 2012; 51: 10751-5.
- Kim J, Lee J, Lee YM, Pramanick S, Im S, Kim WJ. Andrographolide-loaded polymerized phenylboronic acid nanoconstruct for stimuli-responsive chemotherapy. *J Control Release*. 2017; 259: 203-11.
- Cho H, Cho YY, You HB, Han CK. Nucleotides as nontoxic endogenous endosomolytic agents in drug delivery. *Adv Healthc Mater*. 2014; 3: 1007-14.
- Cho H, Lee YJ, Bae YH, Kang HC. Synthetic polynucleotides as endosomolytic agents and bioenergy sources. *J Control Release*. 2015; 216: 30-6.
- BA W, M C, MP J, DL B. Dysregulated pH: A perfect storm for cancer progression. *Nat Rev Cancer*. 2011; 11: 671-7.
- Zhang X, Lin Y, Gillies RJ. Tumor pH and its measurement. *J Nucl Med*. 2010; 51: 1167-70.
- Kim J, Lee YM, Kim H, Park D, Kim J, Kim WJ. Phenylboronic acid-sugar grafted polymer architecture as a dual stimuli-responsive gene carrier for targeted anti-angiogenic tumor therapy. *Biomaterials*. 2016; 75: 102-11.
- Dowlut M, Hall DG. An improved class of sugar-binding boronic acids, soluble and capable of complexing glycosides in neutral water. *J Am Chem Soc*. 2006; 128: 4226-7.
- Bo F, Lin K, Chen L, Ping S, Jin M, Wang Q, et al. Systemic siRNA delivery with a dual pH-responsive and tumor-targeted nanovector for inhibiting tumor growth and spontaneous metastasis in orthotopic murine model of breast carcinoma. *Theranostics*. 2017; 7: 357-76.
- Guo Q, Zhang T, An J, Wu Z, Zhao Y, Dai X, et al. Block versus Random amphiphilic glycopolymer nanoparticles as glucose-responsive vehicles. *Biomacromolecules*. 2015; 16: 3345.
- Li J, Dirisala A, Ge Z, Wang Y, Yin W, Ke W, et al. Therapeutic vesicular nanoreactors with tumor-specific activation and self-destruction for synergistic tumor ablation. *Angew Chem*. 2017; 56: 14025-30.
- Broaders KE, Grandhe S, Frechet JM. A biocompatible oxidation-triggered carrier polymer with potential in therapeutics. *J Am Chem Soc*. 2011; 133: 756-8.
- Xin W, Huang T, Wang C, Zhang J, Wei W, Jiang X. Phenylboronic acid-mediated tumor targeting of chitosan nanoparticles. *Theranostics*. 2016; 6: 1378-92.
- Jeong JY, Hong EH, Lee SY, Lee JY, Song JH, Ko SH, et al. Boronic acid-tethered amphiphilic hyaluronic acid derivative-based nanoassemblies for tumor targeting and penetration. *Acta Biomater*. 2017; 53: 414.

28. Zhou Z, Li H, Wang K, Guo Q, Li C, Jiang HL, et al. Bioreducible cross-linked hyaluronic acid/calcium phosphate hybrid nanoparticles for specific delivery of siRNA in melanoma tumor therapy. *ACS Appl Mater Interfaces*. 2017; 9: 14576-89.
29. Ji M, Ping L, Nan S, Liu L, Hong P, Wang C, et al. Sialic acid-targeted nanovectors with phenylboronic acid-grafted polyethylenimine robustly enhance siRNA-based cancer therapy. *ACS Appl Mater Interfaces*. 2016; 8: 9565-76.
30. Incani V, Lavasanifar A, Uludağ H. Lipid and hydrophobic modification of cationic carriers on route to superior gene vectors. *Soft Matter*. 2010; 6: 2124-38.
31. Egawa Y, Seki T, Takahashi S, Anzai J-i. Electrochemical and optical sugar sensors based on phenylboronic acid and its derivatives. *Mater Sci Eng C*. 2011; 31: 1257-64.
32. Peng Q, Zhong Z, Zhuo R. Disulfide cross-linked polyethylenimines (PEI) prepared via thiolation of low molecular weight PEI as highly efficient gene vectors. *Bioconj Chem*. 2008; 19: 499.
33. Gao W, Liang Y, Peng X, Hu Y, Zhang L, Wu H, et al. In situ injection of phenylboronic acid based low molecular weight gels for efficient chemotherapy. *Biomaterials*. 2016; 105: 1-11.
34. Zhang W, Kang J, Li P, Liu L, Wang H, Tang B. Two-photon fluorescence imaging of sialylated glycans in vivo based on a sialic acid imprinted conjugated polymer nanoprobe. *Chem Commun*. 2016; 52: 13991-4.
35. Zhao D, Xu J, Xiaoqing YI, Zhang Q, Cheng SX, Zhuo RX, et al. A pH-activated targeting drug delivery system based on the selective binding of phenylboronic acid. *ACS Appl Mater Interfaces*. 2016; 8: 14845.
36. Meng Z, Zhong Y, Meng F, Rui P, Zhong Z. Lipoic acid modified low molecular weight polyethylenimine mediates nontoxic and highly potent in vitro gene transfection. *Mol Pharm*. 2011; 8: 2434-43.
37. Beloor J, Choi CS, Nam HY, Park M, Kim SH, Jackson A, et al. Arginine-engrafted biodegradable polymer for the systemic delivery of therapeutic siRNA. *Biomaterials*. 2012; 33: 1640.
38. Maeda H, Wu J, Sawa T, Matsumura Y, Hori K. Tumor vascular permeability and the EPR effect in macromolecular therapeutics: a review. *J Controlled Release*. 2000; 65: 271-84.